Atmos. Chem. Phys. Discuss., 10, 453–489, 2010
www.atmos-chem-phys-discuss.net/10/453/2010/
© Author(s) 2010. This work is distributed under
the Creative Commons Attribution 3.0 License.

Atmospheric Chemistry and Physics Discussions

This discussion paper is/has been under review for the journal Atmospheric Chemistry and Physics (ACP). Please refer to the corresponding final paper in ACP if available.

Atmospheric transport of persistent semi-volatile organic chemicals to the Arctic and cold condensation at the mid-troposphere – Part 1: 2-D modeling in mean atmosphere

J. Ma

Air Quality Research Division, Environment Canada. 4905 Dufferin Street, Toronto, Ontario M3H 5T4, Canada

Received: 26 August 2009 – Accepted: 21 December 2009 – Published: 12 January 2010

Correspondence to: J. Ma (jianmin.ma@ec.gc.ca)

Published by Copernicus Publications on behalf of the European Geosciences Union.

Abstract

In the first part of this study for revisiting the cold condensation effect on global distribution of semi-volatile organic chemicals (SVOCs), the atmospheric transport of SVOCs to the Arctic at the mid-troposphere in a mean meridional atmospheric circulation over Northern Hemisphere was simulated by a two-dimensional atmospheric transport model. Results show that under the mean meridional atmosphere the long-range atmospheric transport of SVOCs from warm latitudes to the Arctic occurs primarily at the mid-troposphere. Accordingly, the cold condensation of the chemicals is likely also to take place at the mid-troposphere over a source region of the chemicals in warm low latitudes. We demonstrate that the temperature dependent vapour pressure and atmospheric degradation rate of SVOCs exhibit similarities between lower atmosphere over the Arctic and the mid-troposphere over a tropical region. Frequent occurrence of atmospheric ascending motion and convection over warm latitudes carry the chemicals to a higher altitude where some of these chemicals may condense/partition to particle or aqueous phase through the interaction with atmospheric aerosols, cloud water droplets and ice particles, and become more persistence in the lower temperatures. Stronger winds at the mid-troposphere then convey the condensed chemicals to the Arctic where they are brought down to the surface by large-scale descending motion and wet deposition. Using calculated water droplet-air partitioning coefficient of several persistent organic semi-volatile chemicals under a mean air temperature profile from the equator to the North Pole we propose that clouds are likely important sorbing media for SVOCs and pathway of the cold condensation effect and poleward atmospheric transport. The role of deposition and atmospheric descending motion in the cold condensation effect over the Arctic was also discussed.

ACPD

10, 453–489, 2010

1 Introduction

Enrichment of semi-volatile organic pollutants (SVOCs) at higher latitudes and the Arctic have been stimulating extensive studies in the scientific community since the 1980s (Goldberg, 1975; Ottar, 1981; Rahn and Heidam, 1981; Macdonald et al., 2000; Meijer et al., 2004). The ability for a specific chemical to travel from its source to the Arctic and be deposited there depends on the physical-chemical properties of the chemical itself, the pathway it takes to move towards the north, the environment and climate pattern along that path. A widely accepted and cited hypothesis that explains the accumulation and atmospheric transport of SVOCs in northern environments is the global distillation effect, proposed originally by Goldberg (1975). Other terminologies have been also used to describe the similar process, e.g., "cold condensation" (Ottar, 1981), and "cold tripping" (Rahn and Heidam, 1981). The northward transport and accumulation of SVOCs have been explored in a number of studies examining latitudinal trends in concentration and composition of SVOCs (Wania and Mackay, 1993, 1996; Mackay and Wania, 1995; Macdonald et al., 2000; Meijer et al., 2003). This notion of contaminant transport has been further developed into the concept of latitudinal fractionation, a process in which certain components of the original mixture of substances are preferentially transported and accumulated in environmental media at higher latitudes, thereby resulting in a change in the mixture's composition (Stow, 2005).

There are various definitions on the global distillation/cold condensation effect and similar processes. One of explanations, adopted by a document of the UNEP (United Nation Environment Programme), states that: "*There is a systematic transfer of these chemicals from warmer to colder areas through the process of global distillation. The pollutants evaporate from soils in warm areas such as the tropics, are transported as vapour around the globe, and condense over cold areas as toxic snow or rain*" (http://earthwatch.unep.net/toxicchem/pops.php).

These popular statements by the UNEP appear to treat the atmosphere as a two-dimension medium, as the statements anticipate that SVOCs condense *only* in cold

ACPD
10, 453–489, 2010

high latitudes. This may lead to a misinterpretation that the poleward atmospheric transport, chemical phase change, and deposition of SVOCs occur near the surface. The potential effect of global large-scale vertical motion on the cold condensation appeared not dealt with. For those persistent SVOCs subject to long-range transport (LRT), a key point is: in what manner will these chemicals be migrated to the polar region? The atmosphere is a three dimensional mobile medium, so is the atmospheric motion. The poleward atmospheric transport of SVOCs must be associated with changes in the meridional atmospheric circulations. From a meteorological perspective, the mean meridional atmospheric circulations and the surface friction appear not to favour the LRT to the Arctic at a lower atmospheric level or within the atmospheric boundary-layer. The atmospheric transport of a chemical occurs most efficiently at a higher elevation rather than near the surface where strong surface friction and turbulence quickly disperse the air concentration of the chemical. Clearly, the free atmosphere is the most efficient pathway for the LRT of a chemical, as demonstrated by numerical investigations of episodic LRT event of toxaphene and lindane (Ma et al., 2005; Zhang et al., 2008).

Abundant field measurements have shown increasing of SVOCs over high mountains associated with declining of air temperature, designated as mountain cold trapping (Calamari et al., 1991; Blais et al., 1998; van Drooge et al., 2004; Wania and Westgate, 2008; MONARPOP, 2009). One may expect that the cold condensation process can also occur at higher atmosphere altitudes in a similar manner as that in the Arctic and high mountains. Under the lower air temperature regime in the Arctic a chemical may condense, adsorb, or partition onto soil, vegetation, water, aerosols, snow and ice (Wania and Mackay, 1993). At a higher atmosphere, however, there exist no as many sorbing media as those in the Arctic. The major pathways for the cold condensation at the mid-troposphere would differ somewhat with the Arctic cold trapping. The uncertainty poses a challenge to the further understanding of LRT and cold condensation process for SVOCs in the Arctic.

In the first part of the present study a two-dimensional atmospheric transport equa-

CC BY

tion model was employed to simulate the long-range atmospheric transport of SVOCs from the tropical latitudes to the Arctic and the cold condensation effect under a mean meridional atmospheric circulation. In the accompany paper (Zhang et al., 2009) two 3-D atmospheric transport models for SVOCs were used to extend the 2-D atmospheric modeling to 3-D atmospheric simulations for episodic poleward atmospheric transport of SVOCs at the mid-troposphere. Given that α- and γ-hexachlorocyclohexane (HCHs) are the most abundant SVOCs in the Arctic atmosphere and surface waters and subject to LRT due to their strong persistence in environments (Macdonald et al., 2000), they were selected in most modeling investigations in the present study. Although some SVOCs in the Northern Hemispheric oceans also show latitudinal increases towards the Arctic (Wania and Mackay, 1996; Stroebe, et al., 2004), this study will focus on the atmospheric transport in the context of the UNEP's statements on global distillation. We propose that the large-scale atmospheric vertical motion would play an important role in the cold condensation effect. The chemicals are elevated by atmospheric ascending motions from its sources in warm latitudes and delivered at the elevated atmosphere levels by stronger poleward winds to the polar region where they sink by large-scale atmospheric descending motion and atmospheric deposition. The cold condensation can also occur at the mid-troposphere over the warm latitudes where some of the chemicals can condense onto the atmospheric aerosols, clouds water droplets and ice particles. This hypothesis will be demonstrated below.

2 Background mean meridional atmospheric circulation for poleward atmospheric transport

Figure 1 shows a mean air temperature profile over Northern Hemisphere from 1950 through 1980. Using the mean air temperatures collected from the NCEP (National Centers for Environmental Prediction) reanalysis (Kalney et al., 1996), as shown in Fig. 1, we have calculated temperature dependent degradation rate constant in the air (Wania and Mackay, 2000) and vapour pressure of γ-HCH (or lindane), a persis-

tent semi-volatile organochlorine insecticide (Xiao et al., 2004). The results are also presented in Fig. 1. The highest air temperature can be observed at relatively lower atmospheric levels and in tropical and sub-tropical regions between 10°–30° N. The air temperature declines towards higher latitudes and the polar region, and higher atmospheric levels. Accordingly, the temperature dependent degradation rate constant (white solid line) and vapour pressure (black dashed line) exhibit the similar decreasing pattern. For instance, it can be seen that the degradation rate constant of lindane at 500 hPa (5500 m height) over the tropical latitudes is identical to that near the surface at the north of 70° N, and the vapour pressure at the value of 0.001 Pa near the surface of 80° N can be also found below 400 hPa (~7000 m height) over the tropical latitudes. The vapour pressure within the range of 0.001–0.01 Pa lies between 650–400 hPa, about 3600–6000 m height above the sea level, located at the mid-troposphere, in the south of 30° N. The same range of the vapour pressure can be seen near the surface between 60°–80° N.

Figure 2 illustrates a vertical cross-section of the vector winds derived from mean meridional wind (m s^{-1}) and vertical velocity (m s^{-1}) from the equator to the North Pole, averaged over springs from 1950 through 1980 and over the Northern Hemisphere, using the data from the NCEP reanalysis. It shows three well-known meridional atmospheric cells, namely, the Hadley cell, Ferrell cell, and Polar cell, spanning from the equator to the North Pole (Holton, 2004). Based on the classic Hadley cell theory (Holton, 2004), warm air rises near the equator and the tropics, cools as it travels poleward at high altitudes, sinks as cold air, and warms as it travels equator-ward. This renders the poleward atmospheric transport from lower latitudes unlikely to occur at the lower level of the mean meridional atmospheric circulations.

3 Model description and methods

We consider a two-dimensional atmospheric transport (dispersion) equation for a SVOC:

$$\frac{\partial c}{\partial t}+\overline{v}\frac{\partial c}{\partial y}+\overline{w}\frac{\partial c}{\partial z}=\frac{\partial}{\partial z}\left(K_c\frac{\partial c}{\partial z}\right)-\Gamma c \tag{1}$$

where c is the air concentration (pg m^{-3}), z (m) is the vertical coordinate in the atmosphere. In Eq. (1) we have assumed that the y-axis is orientated in the direction of the mean meridional wind $\overline{v}$ and $\overline{u}$=0 (m s^{-1}) and in this direction the horizontal advection dominates the transport of an air pollutant. $\overline{w}$ is the mean vertical velocity (m s^{-1}). K_c (m^2 s^{-1}) in Eq. (1) is the eddy diffusivity for air concentration. Γ (s^{-1}) is an overall decay rate constant accounting for the degradation rate constant in air, the air-to-soil mass transfer, and the flux of a persistent substance to the soil – a function of the substance in the soil (Bennett et al., 1999; Beyer et al., 2000).

Equation (1) is solved numerically and analytically. For steady state ($\partial c/\partial t$=0) of Eq. (1), following Bennett et al. (1999) and Beyer et al. (2000), the overall decay rate constant Γ can be defined as

$$\Gamma=\eta_{\mathrm{A}}+F_{\mathrm{s}}K_{\mathrm{AS}}/z, \tag{2}$$

where η_{A} (s^{-1}) is the first-order degradation rate constant in air, K_{AS} (m s^{-1}) is the mass transfer coefficient from air to soil, F_{s} is expressed as the ratio of the net downward flux to the gross downward flux:

$$F_{\mathrm{s}}=\frac{\eta_{\mathrm{S}}}{\eta_S+K_{\mathrm{SA}}/z_{\mathrm{s}}}, \tag{3}$$

where η_{S} (s^{-1}) is the first-order degradation rate constant in soil, K_{SA} (m s^{-1}) is the mass transfer coefficient from soil to air, and z_{s} is the soil depth.

ACPD
10, 453–489, 2010

For steady state solution, the eddy diffusivity in the neutral atmosphere is defined by (Garratt, 1992; Nieuwstadt, 1983)

$$K_c = \kappa u_* z(1 - z/h), \tag{4}$$

where κ is the von Karman constant (=0.4), u_* ($\mathrm{m\,s^{-1}}$) is the friction velocity. Usually, K_c is designated and used in the planetary boundary layer (PBL). Because the influence of the atmospheric turbulence induced by underlying surfaces on the vertical transfer of a chemical is well beyond the PBL up to 10 km (Nieuwstadt, 1983; Strand and Hoc, 1996), following these literatures we have extended K_c to the free atmosphere at a height of h.

An asymptotic solution to a first order of accuracy of Eq. (1) is (Ma and Daggupaty, 1998)

$$c \approx c_0 \left(\frac{K_{c0}}{K_c}\right)^{1/4} \exp\left[\frac{1}{2}\int_{z0}^{z} \frac{\overline{w}}{K_c} dZ - \int_{z0}^{z} \left(\frac{\Gamma}{K_c}\right)^{1/2} dZ\right]$$
$$\exp\left\{-im\left[(y - y_0) + \frac{1}{2\sqrt{\Gamma}}\int_{z0}^{z} \frac{\overline{v}}{(K_c)^{1/2}} dZ\right]\right\}, \tag{5}$$

where K_{c0} is the eddy diffusivity at the height of $z0$. c_0 is determined from the lower boundary condition: $c(x,z)=c_0$ at $z=z0$. m is a wave number, taken as $m=\pi/4\lambda$, where λ is a horizontal scale of the atmospheric transport of a chemical-laden air, taken as 5000 km in an illustrative discussion in the following section. The real part of Eq. (5) determines the changes in air concentration in the vertical subject to the vertical diffusion and vertical motion. The imaginary part determines the horizontal variation in air concentration subject to horizontal winds and vertical diffusion. The overall decay rate constant appears in both the horizontal and vertical variation terms, suggesting that the air/soil (surface) exchange affects the change in air concentration in the vertical and horizontal.

ACPD
10, 453–489, 2010

The real part solution of Eq. (5) can be written as

$$\Re(c) \approx c_0 \left(\frac{K_{c0}}{K_c}\right)^{1/4} \exp\left[\frac{1}{2}\int_{z0}^{z}\frac{\overline{w}}{K_c}dZ - \int_{z0}^{z}\left(\frac{\varsigma}{K_c}\right)^{1/2}dZ\right] \cos\left\{m\left[\frac{1}{2\sqrt{\varsigma}}\int_{z0}^{z}\frac{\overline{v}}{(K_c)^{1/2}}dZ + (y-y_0)\right]\right\} \quad (6)$$

where $\Re(c)$ indicates the real part of the air concentration defined in Eq. (5). It must be noted that Eq. (6) holds only for the first harmonic of cosine function. Equations 5 and 6 indicate that, with a ground source, the air concentration of semi-volatile chemicals will increase exponentially in the vertical with the atmospheric ascending (upward) motion $\overline{w}>0$, and decrease with the descending motion $\overline{w}<0$.

For the non-steady state ($\partial c/\partial t \neq 0$), instead of using the overall decay rate constant Γ Eq. (1) is coupled with a Level IV fugacity soil model to estimate soil/air exchange, and water/air exchange and ice(snow)/air exchange models (Ma et al., 2003). The equation, is solved numerically by an explicit finite-volume scheme for horizontal advection (Hundsdorfer and Spee, 1995) and a semi-implicit Crank-Nicholson scheme for vertical advection and diffusion (Ma et al., 2003). The eddy diffusivity K_c, instead of using Eq. (4), is parameterized by a non-local vertical diffusion scheme (Ma et al., 2003).

4 Results and discussions

4.1 Steady state 2-D transport

As an illustrative case, we calculated α-HCH air concentration using Eq. (6), driven by the NCEP mean meridional wind and vertical velocity plotted in Fig. 2, averaged over springs of 1950 through 1980 and over the Northern Hemisphere. The use of

the spring mean meridional circulation is because the spring is the season when the poleward atmospheric LRT is strongest (Zhang et al., 2008, 2009), and the circulation also exhibits main characteristics of annual circulation pattern. An annual-averaged meridional atmospheric circulation over 1950–1999 is also applied in 2-D non-steady state modeling as presented below. The resulted air concentration profile of α-HCH, overlaid by wind vectors of $\overline{v}$ and $\overline{w}$, is depicted in Fig. 3. As seen, the higher air concentration corresponds to the updraft of the Hadley cell near the equator (5–10° N) and the region dominated by ascending motions between the Ferrel cell and Polar cell (60–65° N). The tropical convection associated with the updraft of the Hadley cell is so strong that it carries large amount of air concentration up to 100 hPa (15 000 m). The air temperature at that level is as low as −50∼−60 °C, far below the air temperature favouring the condensed phase of a SVOC. Given that the vertical motion displayed in Fig. 2 is averaged over springs from 1950 to 1980, we would expect stronger vertical motions during a sporadic weather event (Ma et al., 2005).

4.2 Non-steady state 2-D transport

Figure 4 displays modeled γ-HCH air concentration profile on day 100 (a), 365 (b) and 730 (c) from the non-steady state numerical solution of Eq. (1), driven initially by a γ-HCH soil residue concentration of 1 ton over a tropical region from 5°–20° N, and the spring mean meridional atmospheric circulation. Because the meridional wind, vertical velocity and air temperature do not change on a daily basis, the mean vector winds and air temperature (black solid line) are superimposed only on Fig. 4a. The air concentration rises from its source in tropical latitudes via the updraft of the Hadley cell. It enters subsequently the major atmospheric transport route to the polar region by southerly winds, laying at the 700–3000 m height during the early period (Fig. 4a). This poleward transport route rises to the 3000 m atmospheric level after about 200 d model integration, as seen in Fig. 4b and c. The mean air temperature at this level is 0 °C over the tropics. The same temperature can be observed near the surface in the sub-Arctic (60° N). The corresponding vapour pressure, shown by black solid lines in

Fig. 4b, at this height and the Arctic ranges from 0.005–0.001 Pa. In Fig. 4b we also plot the modeled spatial trend of the mean soil/air fugacity ratio (f_s/f_a), averaged over the first year of model integration and calculated for the soil layer at 1–10 cm and the air at the height of 10 m. Outgassing ($f_s/f_a>1$) dominates the soil/air exchange in the tropical source region and deposition ($f_s/f_a<1$) occurs over the rest latitudes, especially over the Arctic. Interestingly, the γ-HCH-laden air sinks only over the Arctic by a strong downward motion – a signature of the downdraft of the Polar cell. In contrast, the air concentration is considerably lower near the surface over a broad range from 20–60° N, indicating that the atmospheric transport of the chemical to the Arctic under the mean meridional atmospheric circulation is a "one-hop" pathway (Macdonald et al., 2004).

Although the air concentration over the source region declines due to degradation, the high air concentration remains in the Arctic under lower air temperatures. Figure 5 displays modeled daily air concentration at 100 m height over a five-year period at 30°, 60°, and 80° N, respectively. The lowest air concentration is observed at 30° N, corresponding to a wind divergence below the 700 m height (Fig. 4a). Under the mean meridional circulation the air concentration reaches the highest level at 60° N after 3 weeks from its source over 5–20° N and declines thereafter. Although we only input soil residue at the beginning of model integration, after a continuous decreasing for the first two years, the air concentration at 80° N shows an increasing trend. This increasing trend in the high Arctic reflects the persistence and accumulation of the chemical under lower air temperatures. On the other hand, strong downward atmospheric motion centered in 80° N (Fig. 4a) carries γ-HCH -laden air from higher atmospheric level (mid-high troposphere) to the lower atmosphere, thereby increasing the atmospheric level of the chemical.

Further insight into the poleward atmospheric transport under the mean meridional atmospheric circulation can be gained from 2-D non-steady state modeling of α-HCH and hexachlorobenzene (HCB). Compared with γ-HCH, these two chemicals are more persistence and volatile in environments. Their physical/chemical properties are listed in Table 1. Instead of using the spring mean meridional atmospheric circulation as

CC BY

shown in Fig. 2, in this modeling exercise an annual mean meridional – vertical atmospheric circulation in the Northern Hemisphere, averaged over 1950–1999 using the NCEP reanalysis, was employed to drive the 2-D model. Figure 6 shows modeled daily air concentration of α-HCH and HCB at the 10 m height over a 5 yr period in 15° N and 85° N, respectively. In analogous to the 2-D modeling for γ-HCH, in the first instance we defined again the soil residue concentration of 1 t at each model grid (1° degree of latitude) from 5°–20° N as a source of α-HCH and HCB. As seen, at the tropical source location (15° N), both the chemicals show a decreasing trend due to degradation. Given its stronger persistence and volatility, HCB exhibits higher air concentration than α-HCH. Higher air concentration of HCB is also clearly seen in the high Arctic (85° N), although the both chemicals are delivered to the Arctic under the same atmospheric circulation and the same soil residues. The results provide also modeling evidence for the global fractionation effect, referred to the relative transport efficiencies of the two compounds (Wania and Mackay, 1996; Scheringer et al., 2002). Indeed, the stronger persistence and volatility of HCB (Table 1) led to the highest long-range transport potential of HCB (Beyer et al., 2000) and higher concentration of HCB in the Arctic air (Su et al., 2006).

We further examined the LRT of a SVOC to the Arctic by using the gridded global soil residues of α-HCH in 1980 (Li et al., 2000), the year with the highest global soil residue concentration of α-HCH, which are zonally-averaged over the Northern Hemisphere. The averaged inventory shows two peak values of the soil residues near 32° N and 46° N in the Northern Hemisphere, respectively (Fig. 7). By inputting this soil residue inventory into the 2-D model the model was integrated over a 20 yr period from 1980 to 2000 under the annual mean meridional atmospheric circulation. Figure 8 illustrates the modeled vertical profile of the air concentration of α-HCH for the selected years from 1980–2000. The highest concentrations of the compound correspond to its level in the soils, as seen in Fig. 7. At higher levels of the Arctic atmosphere, the air concentration of α-HCH in 1981 and 1984 exhibits a similar pattern as that of γ-HCH, as shown by Fig. 4, though the different soil residues were used. The higher air concen-

CC BY

trations over the tropical region (from 1981–1984 in Fig. 8) was conveyed largely from one of the major sources near 32° N (Fig. 7) via an equator-ward returning flow of the Hadley cell near the surface (Fig. 2). The figure also clearly shows that, except for the major source region in the mid-latitudes (Fig. 7), relatively higher air concentrations remain in the low atmosphere over the Arctic whereas in the low latitudes the significant level of α-HCH air concentration is no longer identified due partly to its shorter life time in tropical environments. Note that in this modeling exercise we used only the α-HCH soil residue in 1980 whereas this pesticide was still used till the early 1990s (Li et al., 2000). Overall, the model successfully simulated major characteristics of the poleward atmospheric transport and the cold condensation effect of this compound under the mean meridional atmospheric circulation. Given that the global, particularly Asian, emission of γ-HCH (lindane) exhibits a similar spatial distribution as that of α-HCH (Li et al., 2000; Zhang et al., 2008), showing higher emission in mid latitudes, the 2-D atmospheric transport of γ-HCH under the same meridional atmospheric circulation also exhibit the similar spatial pattern as that of α-HCH (results not shown).

4.3 Model verification

By using zonally-averaged soil residues the modeled atmospheric concentrations of α-HCH shown by Fig. 8 were actually the zonal-mean air concentration over the Northern Hemisphere. Thus the modeled air concentration of the selected SVOCs may not be properly compared with monitored air concentration at a single site. Given rather homogeneous distribution of SVOCs in air throughout the Arctic (Wania and Mackay, 1993), it is appropriate to compare the modeled mean air concentration of α-HCH in the Arctic with the measured data collected in the Arctic (Li et al., 2004). Results are presented in Fig. 9. The model appears to underestimate the atmospheric level of α-HCH as compared with the measurements (Fig. 9). The underestimations likely result from ignoring α-HCH emissions after 1980. The modeled temporal trend seems to, however, agree well with the measurements.

Perhaps the only attempt to measure a SVOC at the mid-troposphere was made

by Harner et al. (2005) based on high-volume air samples of HCHs collected during a week in the summer of 2001 at Fraser Valley near the west coast of Canada. They have reported the aircraft measured α-HCH air concentration ranging from 1–61 pg m^3 at the 4400 m height in August of 2001, with the mean air concentration at 23 pg m^{-3} at this atmospheric elevation. This is comparable with our modeled concentration (5–30 pg m^{-3}) at the height of 3000–5000 m in 50° N in 1990 (Fig. 7). In 2000, however, our model concentration at the same level in 50° N declines below 5 pg m^{-3}. This can, again, be attributed to the ignorance of the α-HCH emission data after 1980.

5 Cold condensation/partition at a cold, higher atmosphere

Little is known about the partitioning of SVOCs between gas and condensed phase at the mid and high-troposphere. It is known that many gas phase SVOCs may not be sorbed efficiently to the Arctic aerosols during the warm period of a year (Macdonald et al., 2000). The SVOCs' sorption to aerosols at the mid-troposphere over the warm latitudes is likely also not a very efficient pathway for the gas phase and condensed phases partitioning due partly to lower aerosol concentration at higher atmospheric altitudes. Compared with the Arctic environment where the condensed phases include aerosols, rain, fog, snow, soil, vegetation, water surface ..., there are only a few of (condensed phase) sorbing media in the troposphere. Except for atmospheric aerosols, water droplets and ice particles, formed mostly in clouds, are likely important sorbents at the mid-troposphere. Cloud measurements have shown increasing in concentration of water droplets and ice particles with atmospheric altitudes below the mid-troposphere (Rogers and Yau, 1989; Lawrence and Crutzen, 1998). The uptake of pollutants by cloud ice particles and water droplets has been known to be an important pathway of the pollutants in the atmosphere (Lawrence and Crutzen, 1998). However, the knowledge for the uptake of SVOCs by cloud ice particles and water droplets in the free atmosphere is still poor. Lei and Wania (2004) have discussed organic chemical uptake in the rain droplets and snow. The chemical uptake in the rain droplets

CC BY

takes place by dissolution in the liquid phase and sorption to the droplet surface (Goss, 1994, 1997, 2004; Lei and Wania, 2004). It can be reasonably assumed that the uptake mechanism in the rain droplets is identical to the uptake in cloud water droplets. Thus, the method to compute the partitioning between air and rain droplets of organic chemicals can be directly applied in the estimation of the air-cloud droplet partitioning in clouds. Following Lei and Wania, the air-cloud droplet partitioning, expressed as the ratio between the equilibrium concentrations in the cloud droplets and the gas phase of a chemical, is calculated by

$$K_{\text{Droplet/Air}} = K_{\text{WA}} + 3K_{\text{IA}}/r, \tag{7}$$

where K_{WA} is dimensionless and calculated by $K_{\text{WA}}=RT/H$, T is air temperature (K), R is the ideal gas constant, and r is the radius of a cloud droplet, taken as 1 mm in this study (Lei and Wania, 2004). K_{IA} (m) in Eq. (7) is an interface-air partitioning coefficient, defined as the ratio of the interfacial concentration in units of mol m^{-2} of surface and the gas phase concentration in units of mol m^{-3} of air, computed by (Goss, 1997; Hoff et al., 1995; Wania et al., 1998, 1999),

$$\lg K_{\text{IA}}(T) = \lg K_{\text{IA}}(T_{\text{ref}}) - \frac{\Delta H_{\text{s}}}{R}\left(\frac{1}{T} - \frac{1}{T_{\text{ref}}}\right), \tag{8}$$

where Δ_{s} is the enthalpy of adsorption and T_{ref} is the reference temperature. Figure 10 displays computed vertical profile of $\lg K_{\text{Droplet/Air}}$ of PCB52, HCB and α-HCH in the tropical latitude 10° N. The vertical profile of the mean air temperature, zonally-averaged over Northern Hemisphere and averaged over 1950–1980 is also shown in Fig. 10. The $\lg K_{\text{Droplet/Air}}$ values of the three chemicals exhibit a slow change within the atmospheric boundary-layer (lower troposphere) because of the strong vertical turbulent mixing of air temperature and the chemicals due to the underlying surface fraction and heating, but increase rapidly above the lower troposphere, corresponding to the rapid decline in air temperature. Lei and Wania (2004) suggest that the transition from vapour to aqueous phase occurs at $\lg K_{\text{Droplet/Air}}$ of 5.5–7.5. Our results indicate that,

for PCB52 and HCB, such transition occurs at the height of 7000–9000 m. For α-HCH, the vapour to aqueous phase transition takes place at the 3000–9000 m height, corresponding nicely to the height of the atmospheric transport route from the tropical source region to the Arctic at the mid and high-troposphere (Fig. 8). Because the partitioning at the air-ice interface can be approximated by extrapolating adsorption constants for the air-water interface (Hoff et al., 1995; Wania et al., 1998, 1999), the air–ice particle partitioning is not presented here. An estimation of the uptake of the three chemicals in ice (snow) (Lei and Wania, 2004) shows that the vapour to (snow or ice) aqueous phase transition for the three chemicals occurs at the 5000–9000 m atmospheric heights.

Clouds cover about 60% of the sky and are particularly enriched in tropical and warm latitudes due to frequent occurrence of strong convections (Rogers and Yau, 1989). The atmospheric convections not only carry the warm and humid air to a higher atmosphere level where it condenses to a solid phase thereby forming clouds, but also lift chemicals to the higher altitude. The water droplets and ice particles in clouds may act as major sorbing media and provide an efficient pathway of the cold trapping of SVOCs in the mid-troposphere. It is likely that the partitioning processes between SVOCs and cloud droplets and ice particles are similar to that in snow and ice (Hoff et al., 1995; Wania et al., 1998). The change in size and specific surface area of droplets and ice particles, the height, area, properties, and volume of a cloud may make the issue more complex to be understood. Further studies in understanding the sorption and condensation of SVOCs onto cloud droplets and ice particles are needed.

6 Deposition vs. vertical motion

Because the increased vapour to particle and aqueous phase partitioning in the atmosphere gives rise to an increasing in deposition rate, in the explanation of cold condensation effect the atmospheric deposition of SVOCs has been thought to be of equal importance as their condensation in cold, higher latitudes and the polar region.

CC BY

The atmospheric deposition consists of wet and dry deposition. Dry particle deposition in a neutral atmosphere can be defined by

$$v_d = \frac{\kappa F_{\mathrm{m}}^{1/2}}{\ln \frac{z}{z0} + 2\left(\frac{S_r}{P_r}\right)^{2/3}}, \quad (9)$$

where F_{m} is the surface momentum flux, S_r is the Schmidt number, and P_r is the turbulent Prandtl number, respectively. Given that the logarithmic relationship for air concentration (and wind, air temperature and humidity) applies only in the surface atmospheric boundary-layer (below 100 m in the neutral atmosphere), the surface momentum flux tends to vanish above this layer. Thus, the above expression clearly indicates that dry deposition occurs only within the surface boundary-layer. It turns out that, if a chemical moves and condenses at the mid-troposphere, dry deposition does not contribute to its loading to the surface unless it reaches the surface boundary-layer by other atmospheric processes (e.g., downward motion and wet deposition).

On the other hand, precipitation scavenging takes place in precipitation and fog events at atmospheric levels from surface to high troposphere, resulting in wet deposition. The effect of wet deposition on the vertical profile of the chemical's air concentration can be assessed by adding a scavenging coefficient due to precipitation washout to Eq. (2):

$$\Gamma = \Lambda + \eta_A + F_{\mathrm{s}} K_{\mathrm{AS}}/z. \quad (10)$$

The scavenging coefficient is calculated using the formula

$$\Lambda = K_{\mathrm{WA}} P/h, \quad (11)$$

where P is precipitation rate (mm d^{-1}) and h is the depth of the atmosphere layer (~6000 m). γ-HCH, the substance with relatively low octanol/water partitioning coefficient, is selected in the assessment. Considering that wet deposition and atmospheric

CC BY

descending motion play a similar role that carries the chemical from the air to the surface, it is of interest to compare the contribution of these two processes to the change in γ-HCH concentration in the atmosphere. Figure 11 plots the vertical profile of the computed air concentrations from Eq. (6) subject to the selected descending motion at constant vertical velocity at all atmospheric levels $w = -0.1$, -0.01 and $-0.001\,\mathrm{m\,s^{-1}}$ without precipitation, and subject to the precipitation rate at $P_r = 10$ and $100\,\mathrm{mm\,d^{-1}}$ with zero vertical motion. Computed values of air concentration at the vertical levels are listed in Table 2. At higher atmospheric levels, the wet deposition subject to the precipitation rate at either $10\,\mathrm{mm\,d^{-1}}$ or $100\,\mathrm{mm\,d^{-1}}$ reduces more substantially the air concentration than the descending motion. At the lower atmosphere, the strong descending motion at $0.1\,\mathrm{m\,s^{-1}}$ leads to more substantial decline of γ-HCH level in the atmosphere. It is worth noting that such a strong vertical velocity occurs merely in strong meso-scale convections.

We further add a wet deposition flux to the non-steady state solution of Eq. (1) and assume a daily precipitation rate at $1\,\mathrm{mm\,d^{-1}}$ and $0.5\,\mathrm{mm\,d^{-1}}$ over the Arctic, equivalent to the annual precipitation of 365 mm and 187 mm, respectively. This range of precipitation is comparable with the annual averaged precipitation in the Arctic (Barrie et al., 1992). We then integrate the 2-D model for a five-year period. Figure 12 plots the modeled air concentration of γ-HCH with daily precipitation rate at 0, 0.5 and $1\,\mathrm{mm\,d^{-1}}$ at 80° N at 10 m (a) and 3000 m (b) height, respectively. As shown, responding to the washout by precipitation of 0.5 and $1\,\mathrm{mm\,d^{-1}}$, the air concentration at the 10 m height declines about a factor of 2 to 3 throughout the 5 yr integration period compared with that while wet deposition is not taken into account (Fig. 12a). At a level of the mid-troposphere (3000 m), the scavenging by both the 0.5 and 1 mm daily precipitation rate reduces considerably the atmospheric concentration. It can be seen from Fig. 12 that the daily precipitation rate of 0.5 mm leads to almost one order of magnitude reduction of the air concentration compared with that without wet deposition. The doubling this precipitation rate further yields two orders of magnitude reduction of the air concentration at the mid-troposphere during the modeling integration, suggesting that the wet

CC BY

deposition is a dominant pathway for the cold condensation in the Arctic. Nonetheless, as another atmospheric process that is able to carry persistent chemicals from a higher atmosphere elevation to the Arctic surface, the descending motion likely occurs more frequently than the wet deposition and associates with LRT events of SVOCs.

7 Conclusions

While referring to the classical definition on the global distillation/cold condensation process as cited in the Introduction, one can depict a physical picture of the cold condensation effect under the mean meridional atmospheric circulation based on the result of the present study and in the context of the UNEP's statement. In addition to those necessary conditions for the cold condensation as proposed previously (Wania and Mackay, 1993, 1996; Mackay and Wania, 1995), the cold condensation may occur at the mid-troposphere over a source of SVOCs in lower and warm latitudes. The atmospheric convection and ascending motion in the source region carries the chemicals to the mid-troposphere where rapid decreasing air temperature condenses or partitions some of these chemicals from their gas-phase to particle and aqueous phases, where the chemicals become more persistence under lower temperature, and where stronger winds delive more efficiently the condensed chemicals to the polar region. The continuous descending motion and precipitation scavenging carry subsequently the condensed chemicals to the surface of the Arctic ecosystem. To further demonstrate these speculative deductions, extensive modeling investigations for episodic atmospheric transport events have been also carried out and the results will be reported in an accompanying paper (Zhang et al., 2009).

Acknowledgements. This study is funded by the International Polar Year program: Intercontinental Atmospheric Transport of Anthropogenic Pollutants to the Arctic.

References

Barrie, L. A., Gregor, D., Hargrave, B., Lake, R., Muir, D., Shearer, R., Tracey, B., and Bidleman, T.: Arctic contaminants: sources, occurrence and pathways, Sci. Total Environ., 122, 1–74, 1992.

Bennett, D., Kastenberg, W., and McKone, T. E.: General formulation of characteristic time for persistent chemicals in a multimedia environment, Environ. Sci. Technol., 33, 503–509, 1999.

Beyer, A., Mackay, D., Matthies, M., Wania, F., and Webster, E.: Assessing long-range transport potential of persistent organic pollutants, Environ. Sci. Technol., 34, 699–703, 2000.

Blais, J. M., Schindler, D. W., Muir, D. C. G., Kimpe, L. E., Donaldk, D. B., and Rosenberg, B.: Accumulation of persistent organochlorine compounds in mountains of Western Canada, Nature, 395, 585–588, 1998.

Calamari, D., E., Bacci, S., Focardi, C., Gaggi, M., Morosini, M., and Vighi, M.: Role of plant biomass in the global environmental partitioning of chlorinated hydrocarbons, Environ. Sci. Technol., 25, 1489–1495, 1991.

Garratt, J. R.: The atmospheric boundary layer, Cambridge University Press, Cambridge, UK, 1992.

Goldberg, E. D.: Synthetic organohalides in the sea, Proc. R. Soc. Lond., 189, 277–289, 1975.

Goss, K.-U.: Predicting the enrichment of organic compounds in fog caused by adsorption on the water surface, Atmos. Environ., 28, 3513–3517, 1994.

Goss, K.-U.: Conceptual model for the adsorption of organic compounds from the gas phase to liquid and solid surfaces, Environ. Sci. Technol., 31, 3600–3605, 1997.

Goss, K.-U.: The air/surface adsorption equilibrium of organic compounds under ambient conditions, Crit. Rev. Env. Sci. Tec., 34, 339–389, 2004.

Harner, T., Shoeib, M., Kozama, M., and Li, S. M.: Hexachlorocyclohexanes and endosulfans in urban, rural, and high altitude air samples in the Fraser Valley, British Columbia: evidence for trans-Pacific transport, Environ. Sci. Technol., 39, 724–731, 2005.

Hoff, J. T., Wania, F., Mackay, D., and Gillham, R.: Sorption of non-polar organic vapors by ice and snow, Environ. Sci. Technol., 92, 1982–1989, 1995.

Holton, J. R.: An Introduction to Dynamic Meteorology, Elsevier Academic Press, Burlington, MA, USA, 2004.

Hundsdorfer, W. and Spee, E. J.: An efficient horizontal advection scheme for the modeling of

global transport of constituents, Mon. Weather Rev., 123, 3554–3564, 1995.
Kalney, E., Kanamitsu, M., Kistley, R., et al.: The NCEP/NCAR reanalysis project, B. Am. Meteorol. Soc., 77, 437–471, 1996.
Lawrence, M. G. and Crutzen, P. J.: The impact of cloud particle gravitational settling on soluble trace gas distributions, Tellus B, 50, 263–289, 1998.
Lei, Y. D. and Wania, F.: Is rain or snow a more efficient scavenger of organic chemicals?, Atmos. Environ., 38, 3557–3571, 2004.
Li, Y. F., Scholdz, M. T., and van Heyst, B. J.: Global gridded emission inventory of α-hexachlorocyclohexane, J. Geophys. Res., 105(D5), 6621–6632, 2000.
Li, Y.-F., Macdonald, R. W., Ma, J., Hung, H., and Venkatesh, S.: Historical α-HCH budget in the Arctic Ocean: the Arctic Mass Balance Box Model (AMBBM), Sci. Total Environ., 324, 115–139, 2004.
Ma, J. and Daggupaty, S.: A generalized analytical solution for turbulent dispersion with inhomogeneous wind and diffusion coefficient, Environ. Model. Assess., 3, 239–248, 1998.
Ma, J., Daggupaty, S. M., Harner, H., and Li, Y.: Impacts of lindane usage in the Canadian prairies on the Great Lakes ecosystem, Part 1: Coupled atmospheric transport model and modeled concentrations in air and soil, Environ. Sci. Technol., 37, 3774–3781, 2003.
Ma, J., Venkatesh, S., Li, Y., Cao, Z., and Daggupaty, S.: Tracking toxaphene in the North American Great Lakes basin, Part 2: A strong episodic long-range transport event, Environ. Sci. Technol., 39, 8123–8131, 2005.
Macdonald, R. W., Barrie, L. A., Bidleman, T. F., Diamond, M. L., Gregor, D. J., Semkin, R. G., Strachan, W. M. J., Li, Y. F., Wania, F., Alaee, M., Alexeeva, L. B., Backus, S. M., Bailey, R., Bewers, J. M., Gobeil, C., Halsall, C. J., Harner, T., Hoff, J. T., Jantunen, L. M. M., Lockhart, W. L., Mackay, D., Muir, D. C. G., Pudykiewicz, J., Reimer, K. J., Smith, J. N., Stern, G. A., Schroeder, W. H., Wagemann, R., and Yunker, M. B.: Sources, occurrence and pathways of contaminants in the Canadian Arctic: A review, Sci. Total Environ., 254, 93–236, 2000.
Mackay, D. and Wania, F.: Transport of contaminants to the Arctic: partitioning, processes and models, Sci. Total Environ., 160/161, 25–38, 1995.
Meijer, S. N., Ockenden, W. A., Sweetnam, A., Breivik, K., Grimalt, J. O., and Jones, K. C.: Global distribution and budget of PCBs and HCB in background surface soils: implications for sources and environmental processes, Environ. Sci. Technol., 37, 667–672, 2003.
MONARPOP: Monitoring Network in the Alpine Region for Persistent and Other Organic Pollu-

tants, http://www.monarpop.at, last access: 15 August 2009.
Nieuwstadt, F. T. M.: On the solution of the stationary, baroclinic Ekman-layer equations with a finite boundary-layer height, Bound.-Lay. Meteorol., 26, 377–390, 1983.
Ottar, B.: The transfer of airborne pollutants to the Arctic region, Atmos. Environ., 15, 1439–1445, 1981.
Rahn, K. A. and Heidam, N. Z.: Progress in Arctic air chemistry 1977–1980: a comparison of the first and second symposium, Atmos. Environ., 15, 1345–1348, 1981.
Rogers, R. R. and Yau, M. K.: A short course in cloud physics, 3rd edition, Butterworth-Heinenmann, Woburn, MA, USA, 1989.
Schenker, U., Macleod, M., Scheringer, M., and Hungerbuhler, K.: Improving data quality for environmental fate models: a least-square adjustment procedure for harmonizing physico-chemical properties of organic compounds, Environ. Sci. Technol., 39, 8434–8441, 2005.
Scheringer, M.: Persistence and Spatial Range of Environmental Chemicals: New Ethical and Scientific Concepts for Risk Assessment, Wiley-VCH, Weinheim, Germany, 2002.
Stow, J.: Best Available Scientific Information on the Effects of Deposition of POPs, Northern Contaminants Program, Indian and Northern Affairs Canada, UNECE Convention on Long-range Transboundary Air Pollution, Protocol on Persistent Organic Pollutants, 2005, Task Force on POPs, www.unece.org/env/popsxg/docs/2005/a%20effects%20of%20deposition%2015%2006%2005.pdf, March 2009.
Strand, A. and Hov, O.: A model strategy for the simulation of chlorinated hydrocarbon distributions in the global environment, Water Air Soil Pollut., 86, 283–316, 1996.
Stroebe, M., Scheringer, M., Held, H., and Hungerbühler, K.: Inter-comparison of multimedia modeling approaches: modes of transport, measures of long range transport potential and the spatial remote state, Sci. Total Environ., 321, 1–20, 2004.
Su, Y., Hung, H., Blanchard, P., Patton, G. W., Kallenborn, R., Konoplev, A., Fellin, P., Li, H., Geen, C., Stern, G., Rosenberg, B., and Barrie, L. A.: Spatial and seasonal variations of Hexachlorocyclohexanes (HCHs) and Hexachlorobenzene (HCB) in the Arctic atmosphere, Environ. Sci. Technol., 40, 6601–6607, 2006.
van Drooge, B. L., Grimalt, J. O., Camarero, L., Catalan, L., Stuchlik, E., and Carcia, C. T.: Atmospheric semivolatile organochlorine compounds in European high-mountain areas (central Pyrenees and high Tatras), Environ. Sci. Technol., 38, 3525–3532, 2004.
Wania, F. and Mackay, D.: Global fractionation and cold condensation of low volatility organochlorine compounds in polar regions, Ambio, 22, 10–18, 1993.

Wania, F. and Mackay, D.: Tracking the distribution of persistent organic pollutants, Environ. Sci. Technol., 30, A390–A396, 1996.
Wania, F., Hoff, J. T., Jia, C. Q., and Mackay, D.: The effects of snow and ice on the environmental behaviour of hydrophobic organic chemicals, Environ. Pollut., 102, 25–41, 1998.
Wania, F., Semkin, R., Hoff, J. Y., and Mackay, D.: Modelling the fate of non-polar organic chemicals during the melting of an Arctic snowpack, Hydrol. Process., 13, 2245–2256, 1999.
Wania, F. and Mackay, D.: The Global Distribution Model: A non-steady state multicompartment mass balance model of the fate of persistent organic pollutants in the global environment, Version 1.0, http://www.scar.utoronto.ca/~wania/reports/GloboPOP.pdf (last access: August 2009), 2000.
Wania, F. and Westgate, J. N.: On the mechanism of mountain cold-trapping of organic chemicals, Environ. Sci. Technol., 42, 9092–9098, 2008.
Xiao, H., Li, N., and Wania, F.: Compilation, evaluation, and selection of physical-chemical property data for α-, β-, and β-Hexachlorocyclohexane, J. Chem. Eng. Data, 49, 173–185, 2004.
Zhang, L., Ma, J., Venkatesh, S., Li, Y.-F., and Cheung, P.: Modeling evidence of episodic intercontinental long-range transport of lindane, Environ. Sci. Technol., 42, 8791–8797, 2008.
Zhang, L., Ma, J., Tian, C., and Li, Y.: Atmospheric transport of persistent semi-volatile organic chemicals to the Arctic and cold condensation at the mid-troposphere – Part 2: 3-D modeling of episodic atmospheric transport, Atmos. Chem. Phys. Discuss., 9, 26237–26264, 2009, http://www.atmos-chem-phys-discuss.net/9/26237/2009/.

Table 1. Physical/chemical properties of HCB and α-HCH at air temperature of 20°–25 °C*.

	HCB	α-HCH	γ-HCH
Molecular mass (g mol^{-1})	284.8	290.85	291
Molar volume (cm^3 mol^{-1})	166.8	243.6	243
Solid solubility in water (g m^{-3})	1.2	1.0	7.3
log K_{OA}	7.38	7.38	7.74
Degradation half life in soil (day)	2300–3650	800	730
Degradation lifetime in air (day)	730–940	15–120	90
Henry's law constant (Pa m^3 mol^{-1})	131	0.872	0.309

* From Schenker (2005); Xiao et al., (2004)

Table 2. Modeled γ-HCH air concentration at different vertical levels using Eqs. (6) and (8) subject to different vertical velocity w ($m\,s^{-1}$) and precipitation rate P ($mm\,d^{-1}$).

	Air concentration ($pg\,m^{-3}$)				
z (m)	w=0.001 P=0	w=0.01 P=0	w=0.1 P=0	P=10 w=0	P=100 w=0
1.5	58.4	54.8	28.6	54.4	45.7
10	36.3	34.0	17.6	30.6	20.6
20	30.5	28.5	14.7	24.0	13.9
30	27.5	25.7	13.3	20.6	10.6
50	24.2	22.6	11.7	16.7	7.2
100	20.3	19.0	9.8	12.0	3.7
500	13.5	12.6	6.3	4.1	0.3
1000	11.5	10.7	5.2	2.0	0.0
1500	10.5	9.7	4.5	1.1	0.0
2000	9.8	9.1	4.0	0.7	0.0
3000	9.2	8.3	3.3	0.2	0.0
4000	8.9	7.9	2.5	0.1	0.0
5000	8.8	7.5	1.5	0.0	0.0
6000	9.0	6.8	0.4	0.0	0.0

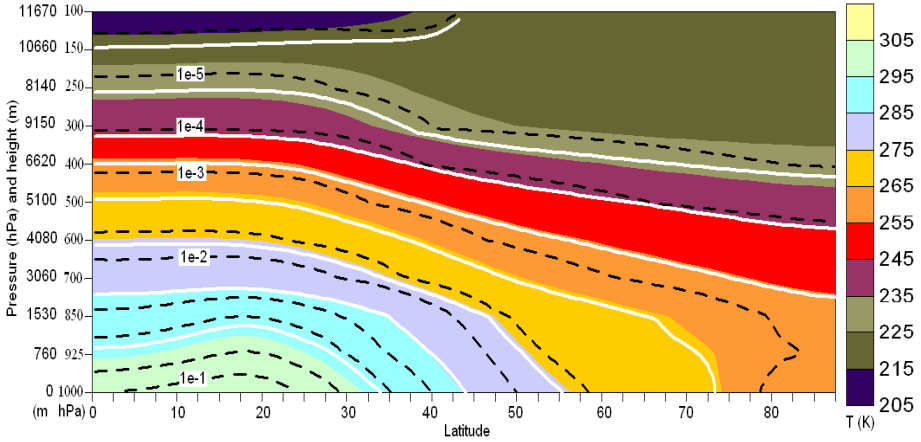

Fig. 1. Vertical profile of zonal-averaging air temperature (color-contoured) over Eurasia (0–140° E) from 1950 through 1980. White solid line indicates the temperature-dependent first order degradation rate of γ-HCH and black dashed line stands for vapour pressure of γ-HCH. The change in the degradation rate is determined by temperature fluctuation and OH radical concentration, defined as $K_e = K_v \cdot [OH] \cdot 1.0 \times 10^6 \cdot \exp[(\Delta E/R) \cdot (1/T_v - 1/T_e)]$, where K_e is the modified reaction (degradation) rate, K_v is the reference degradation rate constant ($m^3\,mol^{-1}\,s^{-1}$), OH is the concentration of hydroxyl radicals in the air (Wania and Mackay, 1996), ΔE is the activation energy ($J\,mol^{-1}$), R is the gas law constant ($J\,mol^{-1}\,K^{-1}$), and T_e and T_v are ambient and reference temperature, respectively. On y-axis the vertical height (m) corresponds to pressures, calculated using the constant air density ρ and the hydrostatic relationship $dp/dz = -\rho g$, where g is the acceleration due to gravity.

ACPD
10, 453–489, 2010

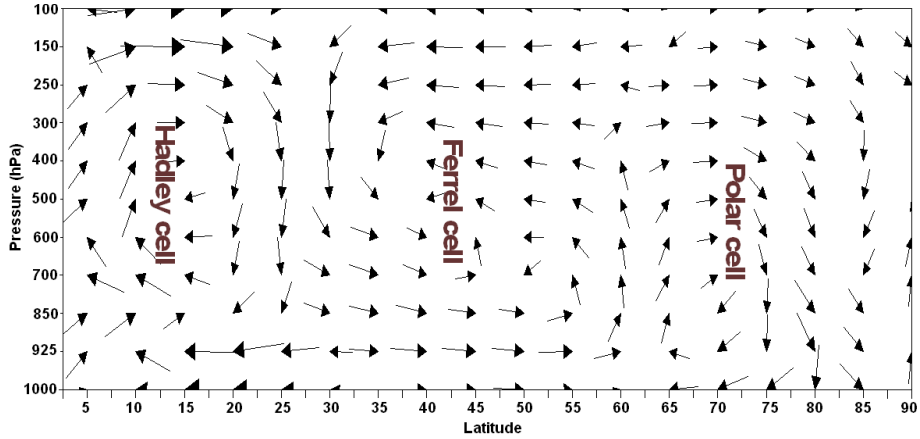

Fig. 2. Vertical profile of vector winds, derived from zonal-averaging meridional wind ($m\,s^{-1}$) and vertical velocity ($m\,s^{-1}$), spanning from the equator to the North Pole, averaged over springs from 1950 through 1980 and over the Northern Hemisphere. In presentation, vertical velocity has been multiplied by 100.

ACPD
10, 453–489, 2010

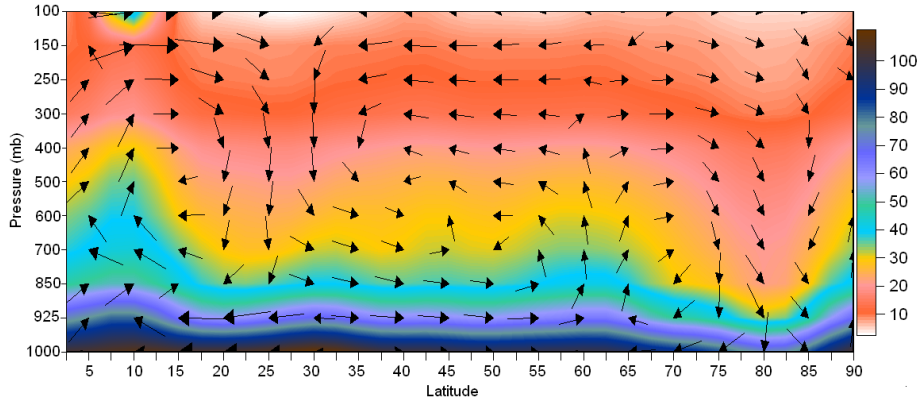

Fig. 3. Vertical profile of computed α-HCH air concentration using Eq. (6), superimposed with the vector winds of v and w component shown in Fig. 2. In the presentation of the vector winds, the vertical velocity w is multiplied by 100.

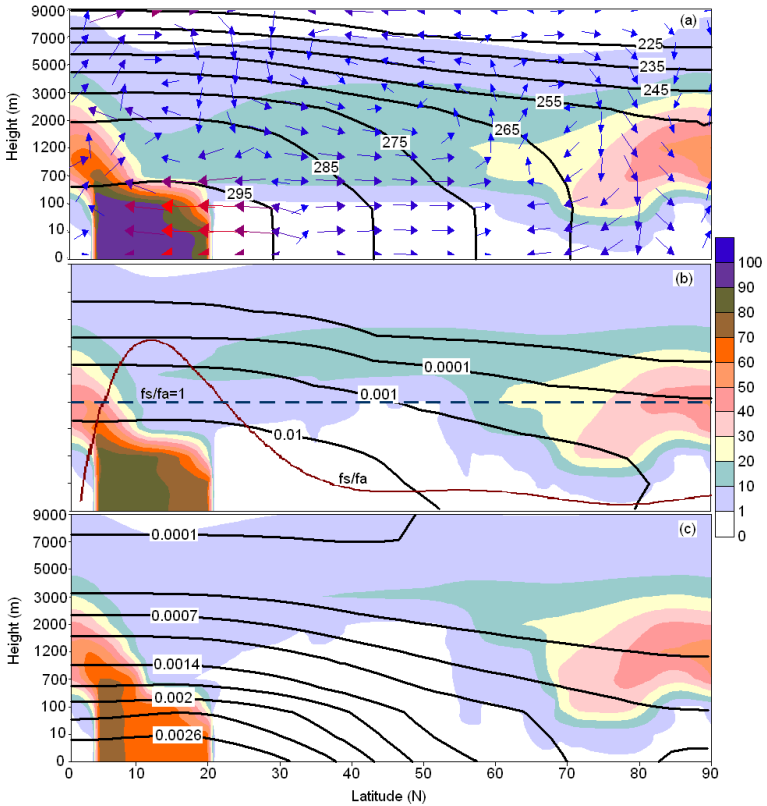

Fig. 4. Vertical cross section of modeled γ-HCH air concentration on day 100 **(a)**, day 365 **(b)** and day 730 **(c)**. Air concentration is superimposed by mean vector winds and air temperature, averaged over 1950–1980 and over the Northern Hemisphere (a), temperature dependent vapour pressure (black solid line) and the trend of annual averaged soil/air fugacity ratio (deep red solid line, dish line indicates f_s/f_a=1) (b), and Henry's law constant (c) of γ-HCH. In the presentation of the vector winds, the vertical velocity w is multiplied by 100.

ACPD
10, 453–489, 2010

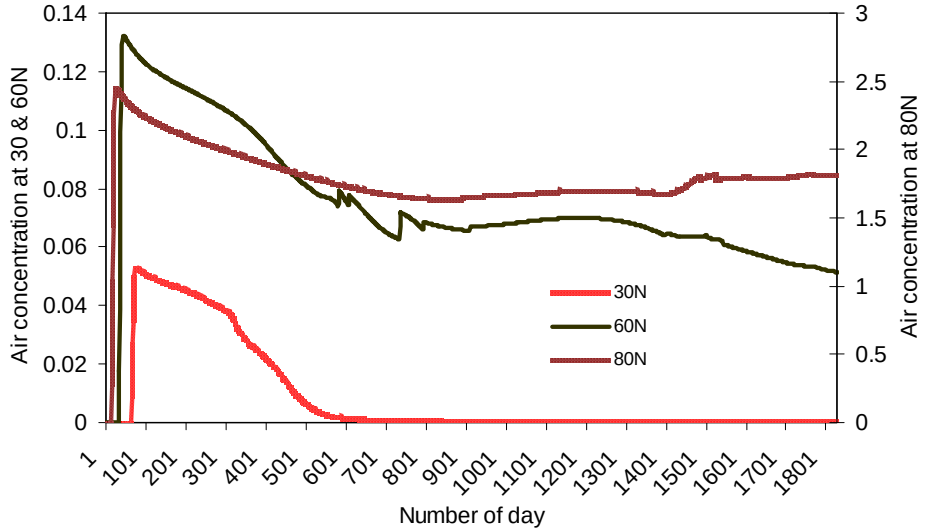

Fig. 5. Daily time series of modeled γ-HCH air concentration at 30°, 60° and 80° N over a 5 yr period.

ACPD
10, 453–489, 2010

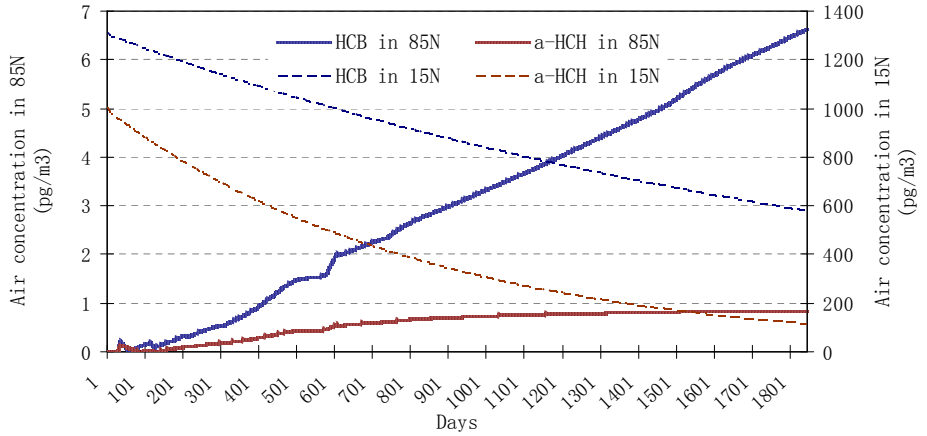

Fig. 6. Modeled daily air concentration of α-HCH and HCB at the 10 m height during a 5 yr period in 15° N and 85° N, respectively.

ACPD
10, 453–489, 2010

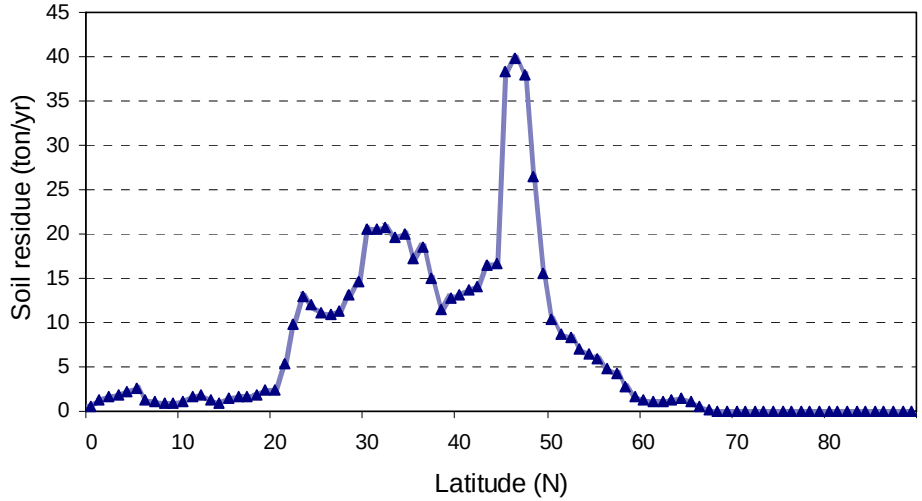

Fig. 7. Mean α-HCH soil residue concentration (ton yr^{-1}) in 1980, zonally-averaged over the Northern Hemisphere.

ACPD
10, 453–489, 2010

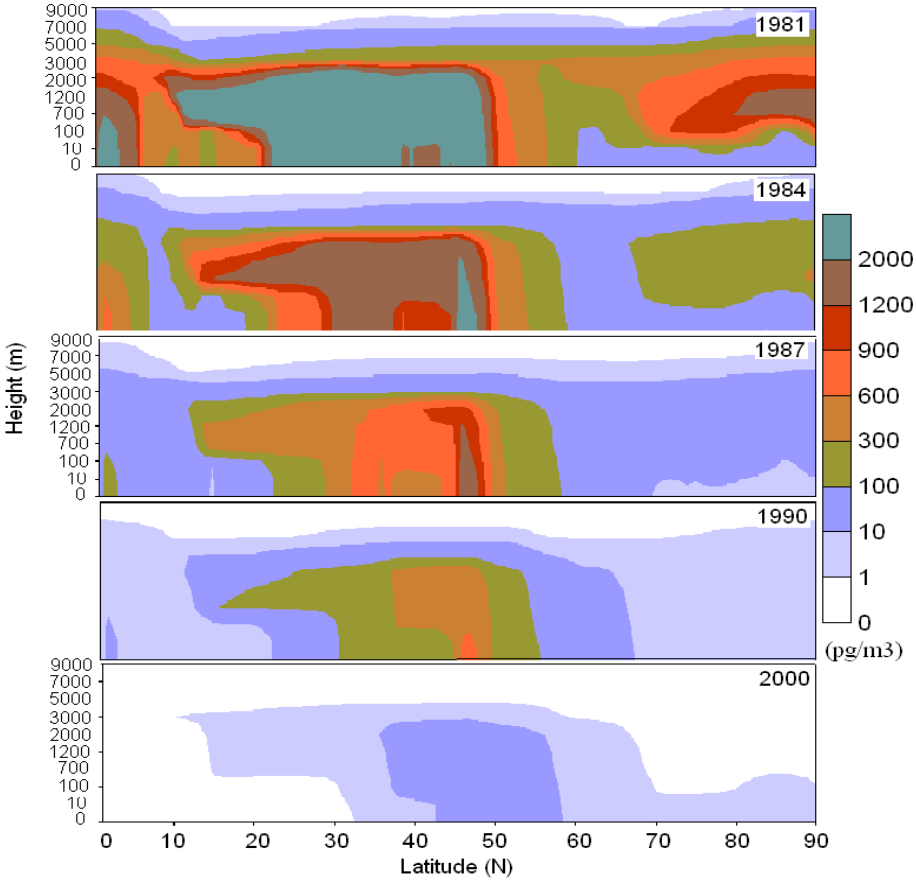

Fig. 8. Vertical cross section of modeled α-HCH air concentration (pg m^{-3}) from 1981 to 2000 using the mean soil residue over the Northern Hemisphere in 1980 (Fig. 7).

ACPD
10, 453–489, 2010

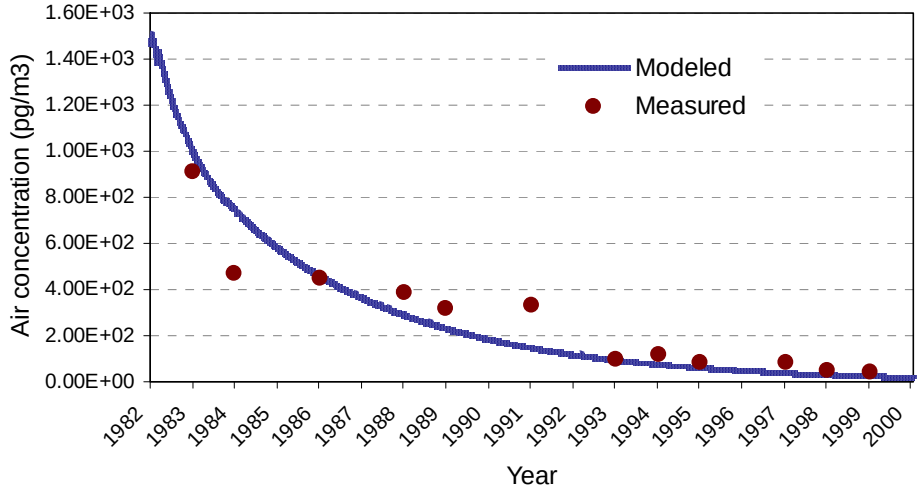

Fig. 9. Modeled and measured atmospheric concentration of α-HCH averaged over the Arctic.

ACPD
10, 453–489, 2010

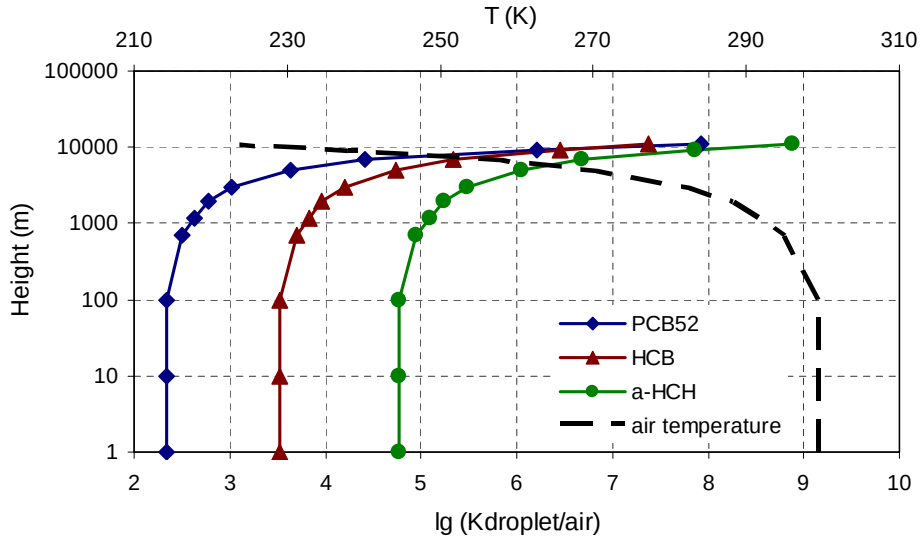

Fig. 10. Vertical profile of temperature dependent air-cloud droplet partitioning $\lg K_{\text{Droplet/Air}}$ for PCB52, HCB and α-HCH at 10° N. $\lg K_{\text{Droplet/Air}}$ at value of 5.5–7.5 indicates the transition from vapour to aqueous phase. The vertical profile in the zonal-averaged air temperature, averaged over 1950–1980, as shown in Fig. 1, is also presented (black dashed line). The upper x-axis indicates air temperature and lower x-axis indicates $\lg K_{\text{Droplet/Air}}$.

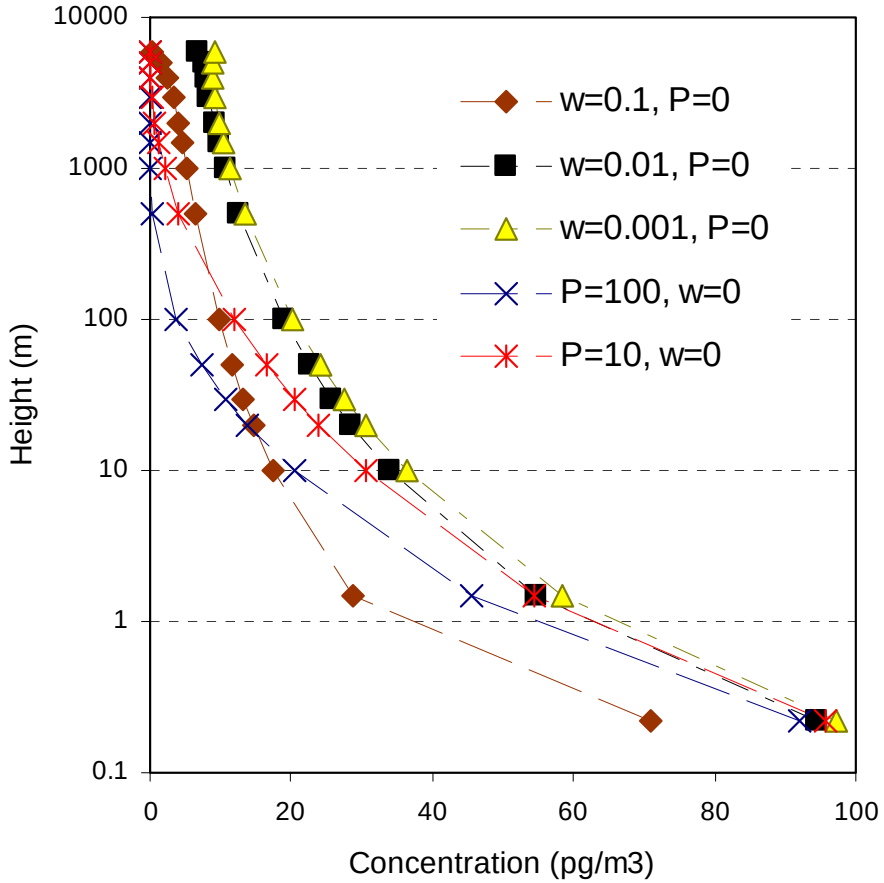

Fig. 11. Vertical profile of computed air concentrations of γ-HCH from Eq. (6) subject to selected descending motion at constant vertical velocity $w = -0.1$, -0.01 and $-0.001\,\mathrm{m\,s^{-1}}$ without precipitation, and subject to the precipitation rate at $P = 10$ and $100\,\mathrm{mm\,d^{-1}}$ without vertical motion.

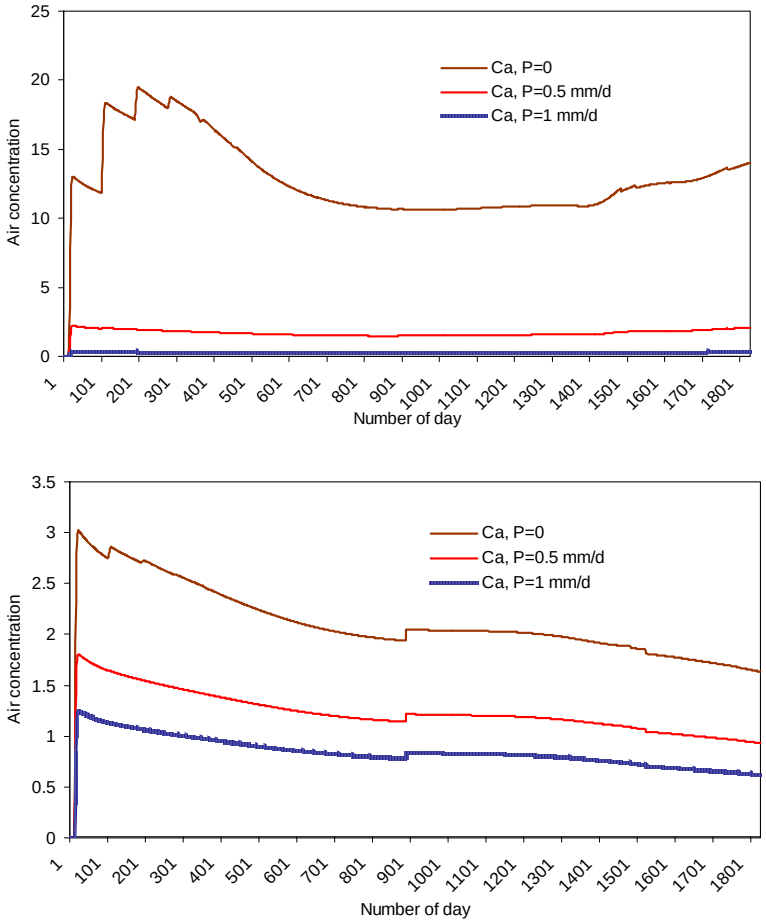

Fig. 12. Daily time series of modeled air concentration (Ca) of γ-HCH at 80° N for a 5 yr period from non-steady state solution of Eq. (1) responding to the precipitation scavenging at daily precipitation rate 0.5 and 1 mm d^{-1} at **(a)** 10 and **(b)** 3000 m height.